Fire Simulation of a Scaled Mass Rapid Transit (MRT) Tunnel

Razieh Khaksari Haddad[1]
Eslam Reda[1]
Mohammad Rasidi Rasani[1]
Cristian Malok Zedan[2]
Zambri Harun[1,*]

[1]*Centre for Integrated Design for Most Advanced Mechanical System,*
Faculty of Engineering and Built Environment,
Universiti Kebangsaan Malaysia,
43600 Bangi, Malaysia

[2]*School of Civil Engineering,*
The University of Queensland,
St Lucia, QLD 4072, Australia

**zambri@ukm.edu.my*

ABSTRACT

The risk of serious accidents increases with the number of road tunnels and their users. Considering the importance of protecting passenger's safety and health in underground tunnels, analysis of the fire flow by the computational fluid dynamics (CFD) simulation is a necessity. The most common ventilation system is the longitudinal ventilation system used in underground tunnels in Malaysia. A major parameter for the designing of this kind of ventilation system is to calculate the "the critical velocity of ventilation" for the system. The value of the critical ventilation velocity is the minimum velocity which can eliminate the backlayering flow, and drive it downstream. This paper carries out a CFD simulation of an unexpected fire occurring in a one-way MRT tunnel with a 2.266 kW fire. This article focuses on the effect of various forced ventilation velocities on the temperature distribution and the stratification of the pollutant to estimate the critical velocity. The results indicate that an increase in the inlet velocity causes the backlayering length decreases. It can also be shown that the average temperature decreases with increasing

ISSN 1823- 5514, eISSN 2550-164X
Received for review: 2017-10-11
Accepted for publication: 2018-07-16
Published: 2018-11-30

longitudinal velocity due to a large amount of entrained fresh air. The results on backlayering and critical ventilation velocity could be utilized by firefighting services designers in preparing the design of such services.

Keywords: *Longitudinal ventilation system; critical velocity; backlayering; CFD*

Introduction

Fires in the road and railway tunnels are particularly dangerous since the amount of combustion products could be lethal to human and can spread over several kilometres along the tunnels. Generally, the fire flow has a very complex structure in a tunnel. Tunnel geometry, inclination, ventilation system capacity, wind pressure and the chemical reaction influence on this physical phenomenon. Consequently, attention about fire safety science of tunnels has increased fire safety science of tunnels have increased significantly because of the rising number of disastrous accidents which leads to tunnel fires and also the increasing number of constructed tunnels. One of the most significant issues in designing effective tunnel ventilation is adequate to control of smoke propagation. Therefore, the behaviours of smoke flow should be investigated appropriately.

The smoke flow forms a column because of the buoyancy force and travels toward the ceiling of the tunnel. As a consequence, the smoke flow propagates toward the right and left directions [1-4], which forms a major problem for user evacuation. Simultaneously, there is a non-linear interaction between turbulence flow, chemical reactions, and the heat of the fire. The smoke remains laminated until it cools down due to the mixed effects of the convective heat transfer to the walls and the mixing between the smoke and the fresh air layer. Therefore, the requirement of a sufficient ventilation system is utmost important to provide an evacuation passage clear of smokes and hot gases. Ventilation may present by natural resource, or by mechanical equipment (longitudinal, semi-transverse or full transverse ventilation systems). The combination of ventilation systems such as utilizing both longitudinal and natural ventilation systems are also common in transportation tunnels. The backlayering event is the smokes produced from the fire which travel in the upstream direction against the direction of the ventilation air and this phenomenon happens if the ventilation velocity is not strong enough to eliminate it [7]. The critical ventilation velocity is the minimum ventilation velocity for preventing the propagation of dangerous fumes of fire by preventing backlayering. This value is a primary criterion when designing tunnel ventilation systems.

Various methods have been performed to analyze the smoke spread and the temperature distribution under different ventilation systems in tunnel fire,

which includes numerical modelling [5, 6, 9 and 12], theoretical analysis and experimental measurement [5,6,9,10 and 12]. The prohibitive cost of experimental tests and the recent positive developments of computational fluid dynamics (CFD) techniques have promoted the use of numerical techniques to simulate tunnel fire scenarios, which is the method we used in this paper. The aim is to investigate the backlayering phenomenon and the impact of ventilation system on it. How the fire heat release rate impact on the critical velocity was studied by Oka and Atkinson [11]. They studied the smoke dispersion using a horizontal model tunnel which was a one-tenth scale of the colliery tunnel. Propane gas burners were utilized as fire sources to control the smoke flow in tunnel fire. The backlayering length, the critical ventilation velocity, and the temperature distribution were analyzed under the ceiling in tunnel fires by means of numerical simulation in the study carried out by He et al. [6]. The longitudinal temperature distribution and the smoke temperature stratification beneath the ceiling under different longitudinal ventilation velocities in tunnel fires are also studied experimentally and numerically [6 and 7]. The relevance between the critical velocity and heat release rate of the fire was investigated by Wu and Bakar [17]. Propane was used as fuel in a horizontal model tunnel to investigate the influence of the tunnel cross-sectional geometry on the critical ventilation velocity numerically and experimentally. The average tunnel hydraulic diameter was used instead of the tunnel height as a characteristic length to defined the dimensionless velocity and the dimensionless heat release rate equations. The experimental results can collapse in a simple a formula. This equation is capable to use for scaling the real tunnels. To understand the fire phenomena precisely, the critical velocity variation for different tunnel dimensions and for various heat source characteristics was investigated by Vauquelin [14] to determinate how tunnel geometry and heat release rate effect on the critical velocity. Also, Gao and Li [5] carried out a numerical simulation to study the critical ventilation velocity in longitudinally ventilated tunnels. They found out that the fuel type and ambient temperature have negligible effects on the critical ventilation velocity based on the CFD results.

Investigating the characteristics of an unexpected fire occurring in a one-way tunnel by a numerical simulation is the objective of this study. Temperature stratification and variation were considered, and the critical ventilation velocity was determined.

Materials and Methods

Physical Model

The geometric structure of this study is shown in Figure 1. In this case, width, w = 0.25 m, height, $H = w$ and $l = 400w$. This length is chosen because it is representative of a typical underground tunnel. This is a scaled-down

dimension for simplicity of calculations. The heat source is modelled as a box with dimension $0.1 \times 0.1 \times 0.1$ m and it is placed at the middle of the tunnel. This fire source dimension produces a heat release rate of 22.6 kW.

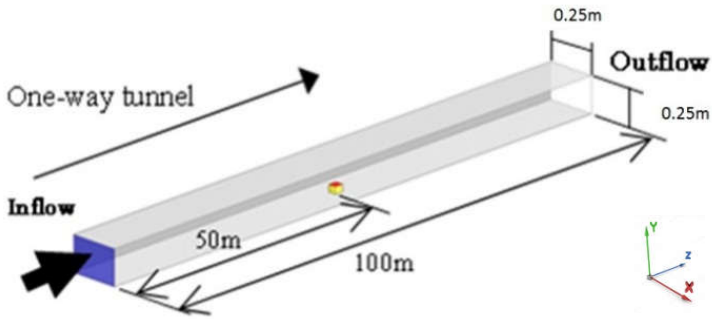

Figure 1 The geometric structure of the field study

Mathematical Model

When the geometry area is determined, the boundary conditions are defined to limit the solution. Then, governing equations including the equations of conservation of mass, momentum, energy, and species are solved simultaneously. In this study, the buoyantBoussinesqPimpleFoam, a solver of OpenFOAM, is used to solve the computational fluid dynamics conservation equations (mass, momentum, and energy), which is a permanent solver for the turbulent, and buoyant flow of incompressible fluids.

- Conservation of mass equation:

$$\frac{\partial \rho}{\partial t} + \frac{\partial (\rho u_i)}{\partial x_i} = 0, \qquad (1)$$

where ρ is the mass density (mass per unit volume), and u is the flow velocity.

- Conservation of momentum equation:

$$\frac{\partial}{\partial t}(\rho u_i) + \frac{\partial}{\partial x_j}(\rho u_i u_j) = \frac{\partial p}{\partial x_i} + \frac{\partial}{\partial x_j}\left[\mu\left[\frac{\partial u_i}{\partial x_j} + \frac{\partial u_j}{\partial x_i} - \frac{2}{3}\delta_{ij}\frac{\partial u_i}{\partial x_i}\right]\right] + \frac{\partial}{\partial x_j}(\rho u_i' u_j') + \rho g, \quad (2)$$

- Conservation of energy:

$$\rho\frac{Dh}{Dt} = \frac{Dp}{Dt} + \nabla.(k\nabla T) + \emptyset. \quad (3)$$

In the above equation, h is the enthalpy, T is the temperature, and Φ is a function representing the dissipation of energy due to viscous effects:

$$\emptyset = \mu\left(2\left(\frac{\partial u}{\partial x}\right)^2 + 2\left(\frac{\partial v}{\partial y}\right)^2 + 2\left(\frac{\partial w}{\partial z}\right)^2 + \left(\frac{\partial v}{\partial x} + \frac{\partial u}{\partial y}\right)^2 + \left(\frac{\partial w}{\partial y} + \frac{\partial v}{\partial z}\right)^2 + \left(\frac{\partial u}{\partial z} + \frac{\partial w}{\partial x}\right)^2\right) + \gamma(\nabla.u)^2. \quad (4)$$

Meshes and Boundary Conditions

In this study, the geometry is divided uniformly in the x – and, y - directions and split into three grading sections in the z-direction. Each of the grading sections is described by three parameters: the fraction of the block length to the total length, the fraction of the cells to the total number of cells, and the grading ratio (size of first cell/size of the last cell). The length of the computational domain, l, is 100 m. Section 1 is the upstream section of the tunnel, its length is 49 m and its grading ratio is 0.0066 and includes 30% of total longitudinal cells. Section 2 is the burner section of length 2 m and it includes 40% of total longitudinal cells with unit grading ratio and Section 3 with the length of 49 m, which covers the downstream region of the tunnel, contains 30% of total longitudinal cells with 150 grading ratio. The reason that a non-uniform grid distribution is used is to reduce the total number of computational cells as well as maintaining a sufficient degree of accuracy for the solution (Figure 2). The total number of cells is 540,000. The results of grid sensitivity tests show that the grid distributions for the tunnel are precise enough. The boundary of the box is assigned a fixed temperature gradient condition. The temperature gradient is set for the fire size (HRR) of 22.6 kW. A uniform fixed longitudinal air velocity is set for the inlet boundary condition while the outlet boundary condition is a zero pressure gradient.

Table 1 Three grading sections in z-direction

	Length, l (m)	Grading ratio	Percentage of total cells (%)
Section 1	49	0.0066	30
Section 2	2	1	40
Section 3	49	150	30

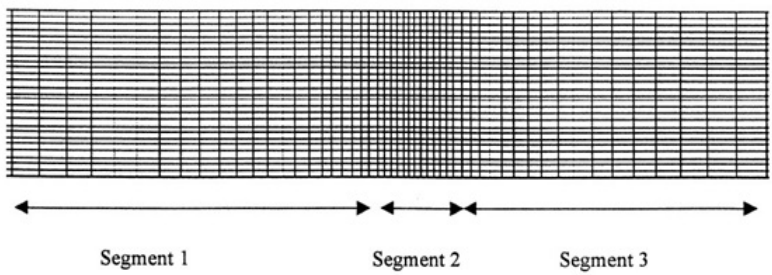

Figure 2 The non-uniform grid distribution

Solution Technique

The temperature and smoke flow fields are simulated in case of the tunnel fire by the CFD package OpenFOAM. In addition, the *k-ε* turbulent model is used for the calculation of flow characteristics includes the temperature of the smoke formed within the tunnel, this is to be discussed later.

The solution of the buoyancy-driven flow is simplified by the Boussinesq's approximation. It ignores density differences in conservation equations except for gravitational term. According to Boussinesq approximation, if ρ is replaced by ρ_0 in Eqs. 1 and 2 except for gravitational term, Eq. 1 is reduced to:

$$\frac{du_i}{dx_i} = 0, \tag{5}$$

and the momentum conservation equation finally is simplified to:

$$\rho_0\left(\frac{\partial u}{\partial t} + u.\nabla u\right) = -\nabla p + \mu_t\nabla^2 u - \rho_0(T - T_0)/T_0 g, \tag{6}$$

here, the density ρ in the gravitational term is expressed by the linear function of the temperature T:

$$\rho \approx \rho_0[1 - \beta(T - T_0)], \tag{7}$$

where β is the thermal expansion coefficient [1/K]. In buoyantBoussinesqPimpleFoam solver, the PIMPLE (semi-implicit method for pressure-velocity coupling) algorithm is used to hold the pressure-velocity coupling.

The flow inside the tunnel is modelled by the standard k-ε turbulence model due to its simplicity and effectiveness. The k-ε turbulence model is a two-equation model to simulate average flow characteristics of the turbulent flow. This model uses two transport variable: k "the turbulence energy", and ε "the rate of viscous dissipation of turbulence energy". The effective viscosity is the sum of the turbulent viscosity and molecular viscosity. In this model, it is estimated that the flow is completely turbulent, and the extraction of the k-ε model is done without concerning the influence of the molecular viscosity. The turbulent effective viscosity in equation 6 is as follows:

$$\mu_t = \rho C_\mu \frac{k^2}{\varepsilon}, \tag{8}$$

Velocity and length scales are solved at each point by the solution of transport equations for k and ε:

$$\frac{\partial}{\partial x_i}(\rho u_i k) = \frac{\partial}{\partial x_i}\frac{\mu}{\sigma_k}\frac{\partial k}{\partial x_i} + G_k + G_b + \rho\varepsilon \tag{9}$$

and

$$\frac{\partial}{\partial x_i}(\rho u_i \varepsilon) = \frac{\partial}{x_i}\frac{\mu}{\sigma_\varepsilon}\frac{\partial \varepsilon}{\partial x_i} + C_1\frac{\varepsilon}{k}G_k + (1 - C_{3\varepsilon})G_b - C_2\rho\frac{\varepsilon^2}{k}. \tag{10}$$

Turbulence is generated according to G_k, where

$$G_k = \mu_t\left(\frac{\partial u_j}{\partial x_i} + \frac{\partial u_i}{\partial x_j}\right)\frac{\partial u_i}{\partial x_i}, \tag{11}$$

and G_b is the generation due to buoyancy:

$$G_b = -g_i \frac{\mu_t}{\rho \sigma_h} \frac{\partial \rho}{\partial x_i}, \quad (12)$$

where σ_h is the turbulent Prandtl number, $\frac{\mu_t C_p}{k}$, and C_1, C_2, C_k, σ_k , and σ_ε are empirical constants, with values, 1.44, 1.92, 0.09, 1.0, and 1.3, respectively [18]. The buoyancy effect is taken into account by $C_{3\varepsilon}$. $C_{3\varepsilon}$ was used equal to 0.20 has been used [15 and 16], and they showed that the modified buoyancy gave better predictions between the measured and predicted results.

Critical Ventilation Velocity

A hot plume produced by heat source moves up above the fire and surrounded by the cold air, which flows into the plume. It forms two layers of hot gases concentration flowing in opposite directions along the ceiling (Figure 3) by reaching the ceiling, and then, it grows till reaching its fully developed stage with constant heat release rate and fill the upstream side of tunnel. A longitudinal flow of air, provided by the ventilation system, is sent inside the tunnel in order to reduce the movement of hot gases through the upstream side and maintain the upstream side of tunnel empty of hot gases. The velocity of hot gases becomes zero in the upstream section of the tunnel at the critical velocity of ventilation with the help of the longitudinal ventilation system.

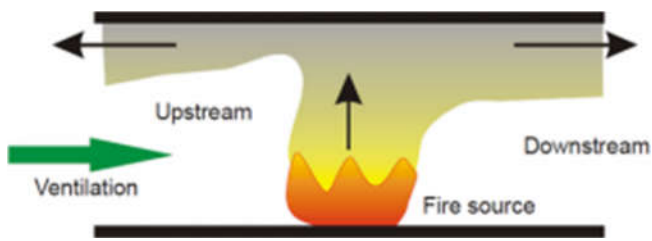

Figure 3 Illustration of the backlayering velocity opposite to the ventilation velocity

The Froude number scaling method is applied to measure the critical velocity, which can be a good estimate for the full-scale tunnel. When the Reynolds number is high enough, turbulent conditions prevail, and buoyancy forces are dominant, this scaling method is often used. The Froude number is a dimensionless number that is the ratio of inertial forces to buoyancy forces. It is defined as:

$$Fr = \frac{U^2}{gL} = \frac{Inertial\ force}{Bouyancy\ force}, \quad (13)$$

where g is the force due to gravity, and u and L are characteristic values of velocity and length, respectively. The validity of Froude modelling has been established over many decades. One of the earliest researchers who used this technique to study the effect of ventilation velocity on fire plumes in ducts was Thomas [13]. Thomas suggested that the flow character depended on the ratio of buoyancy to inertial force over a cross-section of the tunnel. This ratio could be described by a global parameter having the form of a modified Froude number:

$$Fr_m = \left(\frac{gH\Delta T}{U^2 T}\right), \tag{14}$$

where H is the tunnel height, U is the ventilation velocity, and ΔT is the temperature difference with the ambient temperature. It is concluded that when Fr_m is equal to 1 [13], the magnitude of buoyancy force and inertial force are similar, and thus the backlayering does not occur. Then, the relationship between the ventilation velocity and the heat release rate from the fire regards to ΔT and Q, the heat release rate of the fire, was proposed by Thomas [13] is as follows:

$$U_c = a\left(\frac{gQ'}{\rho_0 C_p T}\right)^{1/3}. \tag{15}$$

In the above equation, U_c is the critical ventilation velocity, Q' is convective heat release rate per unit width of the tunnel, ρ_0 is the ambient air density, C_p is the specific heat capacity of air, a is a constant, and T is the smoke temperature. There are a few unclear issues in the current methods of prediction of the critical ventilation velocity. Firstly, the influence of the heat release rate on the critical ventilation velocity and secondly, the effect of the tunnel geometry on the critical velocity. Both problems lead to the issues of the scaling techniques in tunnel fires. The experimental results showed that the critical velocity varied with the tunnel cross-sectional geometry significantly. It was also shown clearly that there are two trends regards to the variation of critical velocity against heat release rate. At low rates of heat release, the critical velocity varies as the one-third power of the heat release rate, however at higher rates of heat release; the critical velocity becomes independent of fire heat release rate [11]. The most recently used model for calculating the critical ventilation velocity is those presented by Oka and Atkinson [11], which is based on their small-scale experimental results. This model considered that the tunnel height influenced on the buoyancy force of the backlayering flow directly.

The experimental results clearly demonstrate that the tunnel width also impacted on the critical velocity as well as the tunnel height. Therefore,

considering the tunnel height as a characteristic length lonely is not suitable. The tunnel hydraulic diameter was proposed by Wu and Bakar [17] as the characteristic length when conducting the dimensionless analysis and presented a dimensionless relationship for critical ventilation velocity and heat release rate, where the tunnel height was replaced with the tunnel hydraulic diameter. They obtained different values of U_{max} and the critical $Q^{"}$ values of 0.4 m/s and 0.2 kW, respectively. It was concluded that the average hydraulic diameter of the tunnel (which includes the effect of both width and height of the tunnel) affected on the dynamic flow of air inside the duct, in comparison with the depending on the height of the tunnel. In this present work, we use the tunnel hydraulic diameter, $\overline{H}$ and replace it with the tunnel height, H, as the characteristic length in the dimensionless analysis. The hydraulic tunnel height is:

$$\overline{H} = \frac{4A}{P}, \tag{16}$$

where A is the cross-section area of the tunnel and P is tunnel perimeter. Thus, the new dimensionless critical ventilation velocity, U_c' and new dimensionless heat release, $Q^{"}$ are defined according to Eqs. 17 and 18.

$$Q^{"} = \frac{Q}{\rho_0 C_p T_0 \sqrt{g\overline{H}^5}}, \tag{17}$$

$$\begin{aligned} U_c' &= 0.40[0.2]^{1/3}[Q^{"}]^{1/3} && \text{for } Q^{"} \le 0.2, \\ U_c' &= 0.4 && \text{for } Q^{"} > 0.2, \end{aligned}$$

Finally, the critical velocity is calculated according to Eq. 19:

$$U_c' = \frac{U_c}{g\overline{H}}. \tag{19}$$

Case Studies

In order to investigate the effect of longitudinal ventilation velocity and finding out the efficient velocity, which can eliminate the backlayering flow, for a constant heat release rate Q, the simulation is run with a selected ventilation velocity and the formation of the back-flow is investigated by comparing the longitudinal velocity and temperature contours in the middle plane (x = 0.125).

Results and Discussions

Grid Sensitivity

Figure 4 illustrates the temperature at the middle y-axis of the tunnel. Three simulations with three different meshes (160,000, 540,000, and 1,280,000) are carried out under the same ventilation velocity and heat release rate. All the simulations were run for a total simulation time of 100 s. It appears that the variation of temperature is not affected notably by the grid after few variations of nodes. As can be seen, the temperature difference between mesh No. 2 with 540,000 nodes and mesh No. 3 with 1,280,000 nodes is less than 2%. So, 540,000 cells were thought to be enough in the present work.

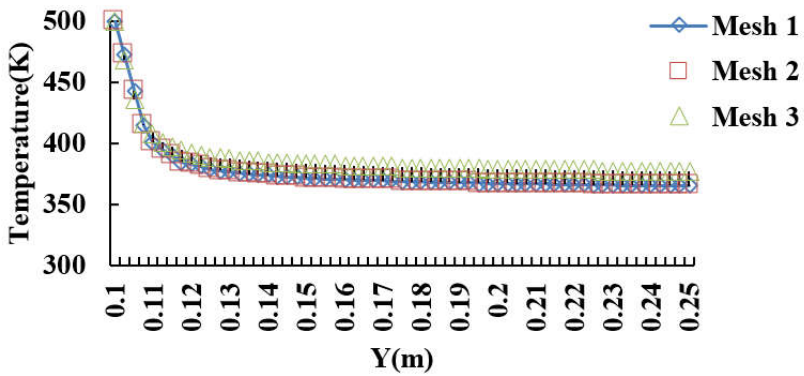

Figure 4 Effect of cell size on vertical temperature profiles

Critical Velocity Investigation

According to the critical velocity formula proposed by Wu and Bakar [17], the calculated critical velocity for 2.266 kW heat release rate based on the dimension of the investigated tunnel is 0.43 m/s. The longitudinal ventilation velocity has a significant impact on the smoke temperature stratification, as shown in Figure 5 and, 6. Comparing graphs of different velocities, the length of backlayering flow was found to decrease by increasing the inlet velocity (Figure 5). At an inlet ventilation velocity (0.4 m/s), the reverse layer is eliminated. Thus, the critical ventilation velocity predicted by CFD is slightly lower than the value calculated by the empirical formula in Eq. 17. For these temperature fields in Figure 6, the temperature is higher in the upstream than the downstream of the heat source. The incoming longitudinal ventilation velocity acts as a barrier, then the heat accumulates behind the ceiling and the local temperature increases. While further away, upstream the barrier, the hot

gases front shears the oppositely coming longitudinal velocity, resulting in more air entrainment and faster temperature decrease. Also, the flow becomes homogeneous i.e. a uniform mixture of ventilation air and hot gases are formed. A combination of the ventilation flow and the hot gases flow and reduce the temperature values.

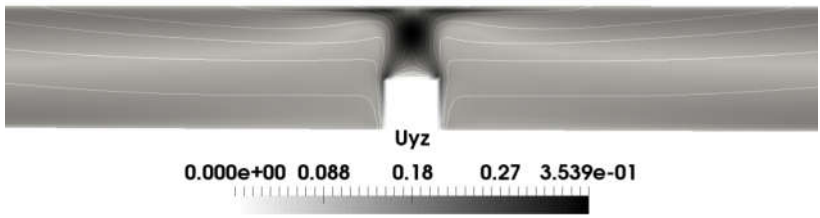

(a)

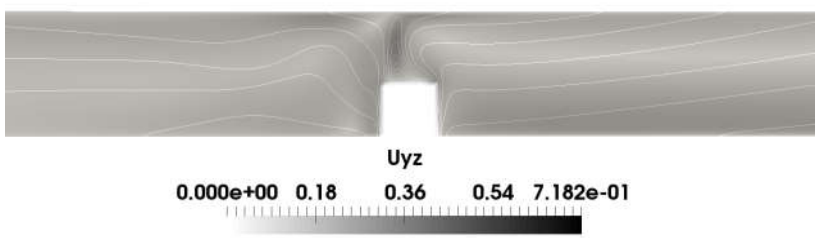

(b)

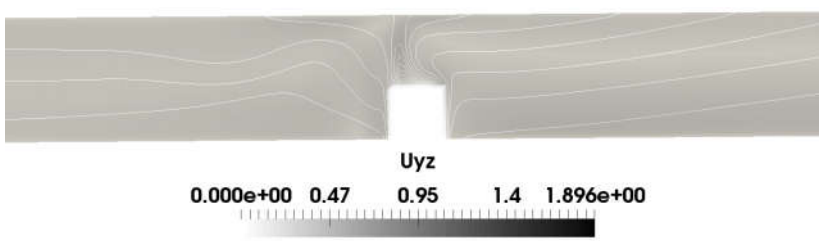

(c)

Figure 5 Velocity contour (m/s) in *y*-*z* plane at $x = 0.125$ plane at different ventilation velocities, (a) $U = 0.0$ m/s, (b) $U = 0.2$ m/s and (c) $U = 0.4$ m/s

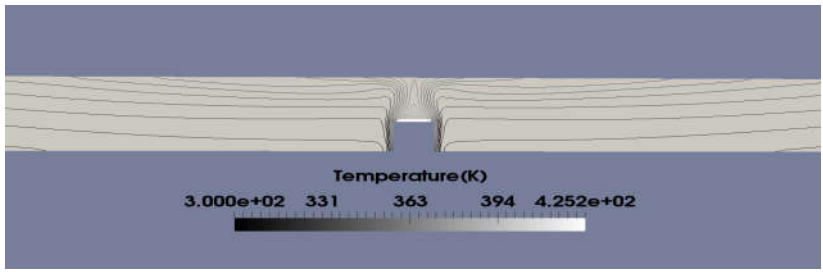

(a)

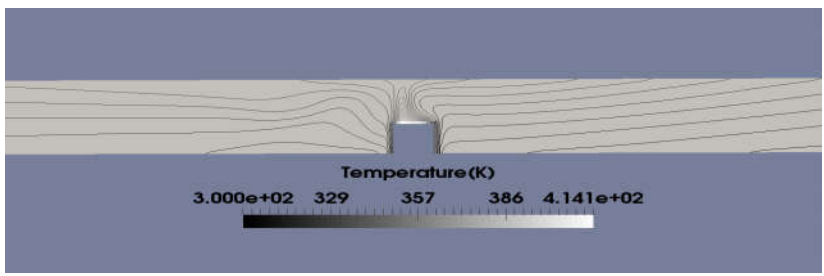

(b)

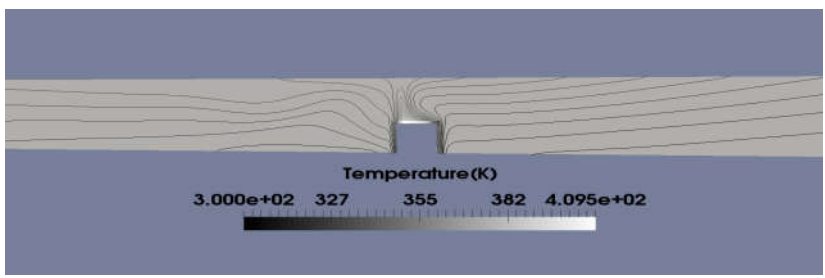

(c)

Figure 6 Temperature contour at $x = 0.125$ plane at different ventilation velocities, (a) $U = 0.0$ m/s, (b) $U = 0.2$ m/s and (c) $U = 0.4$ m/s

Smoke Temperature

Figure 7 shows the hot gases temperature profile along the middle y-axis at the different ventilation velocities investigated. The maximum temperature occurs in the vicinity of the heat source. It can be obtained that when the longitudinal velocity increases, the temperature decreases as a consequence of entraining more fresh air. In other words, heat can be removed from boundaries, temperature decreases, through air entrainment. The maximum temperature of gases is recorded at a zero ventilation velocity. It becomes more than 360 K for 100 seconds. The temperature of hot gases at the same location decreases

by increasing the ventilation velocity and reaches about 330 K at a 0.4 m/s velocity. This figure shows that for higher ventilation velocities, the vertical temperature of hot gases is reduced. This is due to the enhanced entrainment of fresh air into the plume, due to higher longitudinal ventilation velocities, suppresses the back-flow layer.

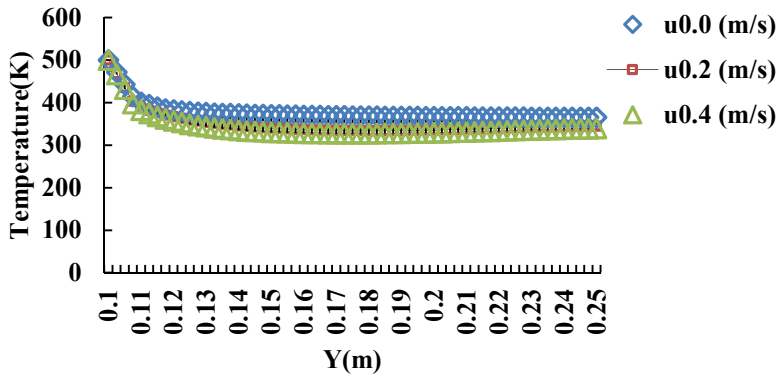

Figure 7 Vertical temperature plot in different longitudinal ventilation velocity

Temperature Stratification

Due to the existence of the longitudinal ventilation flow and the moderation effect of the tunnel walls, the fire plume shape is quite different with the fire plume in free space. The hot gases simulation of the longitudinal air flow is also complex. The smoke flow can take several forms as fluid moves toward the downstream section and when the geometry of the tunnel and, the characteristic of the plume is considered. The steady-state temperature distribution in the hot gases plume section of the downstream section of the tunnel is measured. The longitudinal ventilation velocity has a substantial effect on the temperature diffusion of fire products. Figure 8 gives the temperature contours of the hot gases plume in the centre plane of the tunnel at 0.4 m/s ventilation velocity. As shown in Figure 8, free hot gases plume consists of three distinct regimes. They are:

(1) A continual flow of burning gases, where there is an accelerating flow adjacent to the heat source right above the burner.
(2) An intermittent flame with an approximate flow velocity.
(3) The buoyant plume which its velocity and temperature decrease as the height increases.

The fire plume regime in tunnels is analyzed by the measured temperature contours in the present work. It is clear that the temperature in the persistent flame regime of the critical ventilation velocity situation is greater than 400 K. The temperature in the intermittent regime is between 370 K and 340 K. The buoyant smoke is considered to have a temperature of less than 330 K.

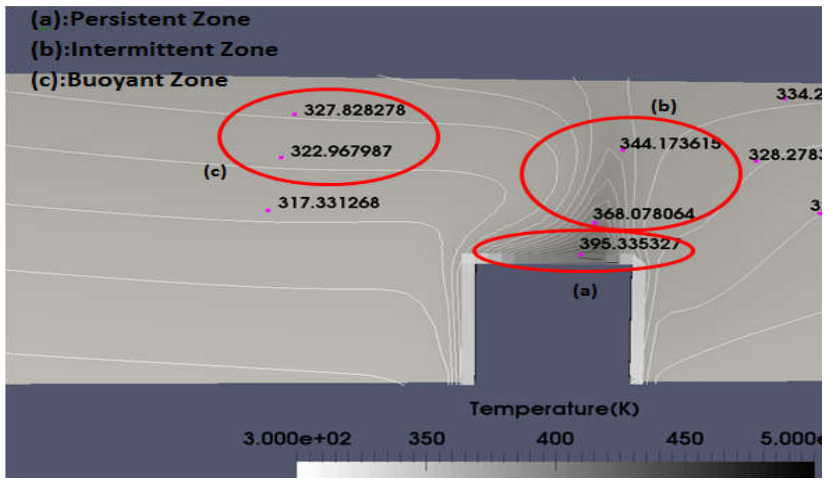

Figure 8 Temperature contour at $x = 0.125$ plane in longitudinal ventilation velocity $U = 0.4$ m/s

Conclusion

In this study, numerical simulations have been carried out to examine the transient effect of the ventilation system in the tunnel. The longitudinal velocity affects the thermal stratification especially by increasing the longitudinal velocity of upper buoyant flow and hence decreasing the hot layer temperature. This study shows that the occurrence of backlayering in tunnel fire could be eliminated at a critical ventilation velocity of 0.4 m/s. The calculated critical velocity by this numerical simulation is 0.4m/s, which is slightly lower than the value obtained from the empirical formula, 0.43m/s. In the design of ventilation strategy for firefighting operations in a channel-like construction, like the MRT tunnels, this value is recommended to be taken into account. It is also found that the temperature of hot gases at the same location decreases by increasing the ventilation velocity and three distinct regimes of

free hot gases plume were derived from numerical simulation. Further study is required to investigate a more accurate representation of the smoke flow in tunnel fire simulations with attention to other parameters like tunnel construction and geometry effects.

Acknowledgements

This work was supported by the Research Fund provided by The Ministry of Higher Education Malaysia via grants FRGS/2016/TK03/UKM/02/1/ and UKM grant AP-2015-003.

References

[1] C.C. Hwang and J.C. Edwards, "The critical ventilation velocity in tunnel fires - a computer simulation," Fire Safety Journal (40), 213– 244 (2005).
[2] H. Ingason and Y.Z. Li, "Model scale tunnel fire tests with longitudinal ventilation," Fire Safety Journal (45), 371–384 (2010).
[3] A. Kashef, N. Bénichou and G. Lougheed, "Numerical modeling and behavior of smoke produced from fires in the Ville-Marie ad L.-H.-La obtained Tunnels," Literature review, NRCC Report IRC-RR-141. (2003).
[4] J.P. Kunsch, "Simple model for control of fire gases in a ventilated tunnel," Fire Safety Journal (37), 67–81 (2002).
[5] R. Gao, and A. Li, "Dust deposition in ventilation and air-conditioning duct bend flows," Energy Conversion and Management. (55), 49–59 (2012).
[6] L.H. Hu, R. Huo and W.K. Chow, "Studies on buoyancy-driven back-layering flow in tunnel fires," Experimental Thermal and Fluid Science (32), 1468–1483 (2008).
[7] L.H. Hu, R. Huo, H.B. Wang, Y.Z. Li and R.X. Yang, "Experimental studies on fire-induced buoyant smoke temperature distribution along tunnel ceiling," Building and Environment (42), 3905–3915 (2007).
[8] L.H. Hu, R. Huo, W. Peng, W.K. Chow and R.X. Yang, "On the maximum smoke temperature under the ceiling in tunnel fires," Tunneling and Underground Space Technology (21), 650–655 (2006).
[9] Y. Huang, X. Gong, Y. Peng, X. Lin and C.N. Kim, "Effects of the ventilation duct arrangement and duct geometry on ventilation performance in a subway tunnel," Tunneling and Underground Space Technology (26), 725 (2011).
[10] D.Huo, R. Zhang and X.L. Zhao, "On the front velocity of buoyancy-driven transient ceiling jet in a horizontal corridor: Comparison of

correlations with measurements," Applied Thermal Engineering (31), 2992 (2011).
[11] Y. Oka and G.T. Atkinson, "Control of smoke flow in tunnel fire," Fire Safety Journal (25), 305-322 (1995).
[12] C.M.K. Se, E.W.M. Lee and A.C.K. Lai, "Impact of location of jet fan on airflow structure in tunnel fire," Tunneling and Underground Space Technology (27), 30 (2012).
[13] P.H. Thomas, "The movement of smoke in horizontal passages against an air flow," Fire Research Station Note (723), Fire Research Station, UK, (1968).
[14] O. Vauquelin, "Parametrical study of the back flow occurrence in case of a buoyant release into a rectangular channel," Experimental Thermal and Fluid Science (29), 725–731 (2005).
[15] P.J. Woodburn and R.E. Britter, "CFD simulation of a tunnel fire * Part 1," Fire Safety Journal (26), 35-62 (1996).
[16] P.J. Woodburn and R.E. Britter, "CFD simulation of a tunnel fire * Part 2," Fire Safety Journal (26), 63-90 (1996).
[17] Y. Wu and M.Z.A. Bakar, "Control of smoke flow in tunnel fires using longitudinal ventilation systems—a study of the critical velocity," Fire Safety Journal (35)4, 363–390 (2000).
[18] H.K. Versteeg, and W. Malalasekera, "An introduction to computational fluid dynamics: The finite volume method." (2007).